Hindawi
Advances in High Energy Physics
Volume 2017, Article ID 7907858, 16 pages
https://doi.org/10.1155/2017/7907858

Research Article

Analysis of Various Projectile Interactions with Nuclear Emulsion Detector Nuclei at ~1 GeV per Nucleon Using Coulomb Modified Glauber Model

N. Marimuthu,[1,2] V. Singh,[1] and S. S. R. Inbanathan[2]

[1]*Department of Physics, Institute of Science, Banaras Hindu University, Varanasi 221005, India*
[2]*Post Graduate and Research Department of Physics, The American College, Madurai 625002, India*

Correspondence should be addressed to V. Singh; venkaz@yahoo.com and S. S. R. Inbanathan; stepheninbanathan@gmail.com

Received 29 June 2017; Accepted 25 September 2017; Published 31 October 2017

Academic Editor: Anna Cimmino

The total nuclear reaction cross section is calculated considering the cases with and without medium effect by employing Coulomb modified Glauber model (CMGM) for interactions of projectiles $^{56}Fe_{26}$, $^{84}Kr_{36}$, $^{132}Xe_{54}$, $^{197}Au_{79}$, and $^{238}U_{92}$ with nuclear emulsion detector (NED) nuclei at around 1 GeV per nucleon incident kinetic energy. These calculated nuclear reaction cross sections are correlated with the different target groups of the NED nuclei. The average value of various parameters is also calculated and compared with the corresponding experimental results. The number of shower particles emitted in an interaction is also calculated and showed good agreement with the experimental result. We observed that the total nuclear reaction cross section increases with increasing the target mass number in case of all the considered projectiles. In addition, it is shown that the average value of reaction cross section with nuclear medium effect is in good agreement with the experimental results for projectiles ^{56}Fe, ^{84}Kr, and ^{132}Xe, although results of projectiles ^{197}Au and ^{238}U are not in agreement with the experimental observations. This study sheds some light on the energy dependence of the nuclear reaction cross section.

1. Introduction

The relativistic heavy-ion collision in the intermediate and high-energy domains has been extensively studied both theoretically and experimentally for a long time [1–6]; this study is highly interesting because of their important application and new research opportunities. In these regions, heavy-ion collision provides us with information to understand the mechanism of nuclear fragmentation, space-time development of hadronic interactions under extreme condition, and formation of exotic nuclei [1, 2]. The photographic nuclear emulsion detector is one of the excellent tools to understand the high-energy interactions because it provides excellent spatial resolution and very high efficiency of charge particle detection over complete solid angle [7–10]. In the heavy-ion collision, the projectile nuclei or hadrons interact with a target nucleus to produce the multiparticles and these particle productions should be considered as two different steps [1]. In the initial step, the interacting projectile nuclei mainly interacts with the primary reaction and completely overlap with the target nucleus and then leave the projectile-target participant region without any further interaction. This process associated with the production of singly charged relativistic particles, that is, shower particles (N_S), which is mainly pions and small mixture of k-mesons, having velocity greater than 0.7 c. In the next step, the produced shower particles may be involved in the rescattering process with target nucleus and knock out the nucleons (proton) from the target nucleus. These particles are called grey particles (N_g). The relative velocity (v/c) of grey particle belongs in between 0.3 c and 0.7 c, that is, ($0.3\,c < \beta < 0.7\,c$) and their kinetic energy ranges from 30 MeV to 400 MeV, that is, ($30 < E < 400$ MeV). Due to the consequence of these two different steps, the hadron production is not an instantaneous process

and it will take certain time, which is said to be creation time [1]. The excited target residuals nucleus comes back to the initial state by losing their energy and attains thermal equilibrium by emitting the nuclear material in the form of fragments. These target fragments are known as black particles (N_b) [11, 12]. These black particles have relative velocities (v/c) and kinetic energies less than 0.3 c and less than 26 MeV, respectively.

The total nuclear reaction cross section (σ_R) is one of the most important physical quantities in the heavy-ion collision. From this reaction cross section, one can extract the fundamental information about the nuclear size and density distribution of protons and neutrons inside the nucleus [18]. Based on the nuclear reaction cross section, one can describe the strong interaction of hadron-nucleus (h-A) and nucleus-nucleus (A-A) interactions. It has application in various research fields, including shielding against heavy-ions coming from the space radiations or accelerators, cosmic ray propagation, and radio-biological effects resulting from clinical exposures [2].

The Glauber Multiple (GM) scattering theory is commonly used to describe the nuclear reaction cross section at high energies. In the high-energy collisions, the GM has been applied successfully and the total nuclear reaction cross section has been extracted [13, 19, 20]. This model has been extended for the study of total nuclear reaction cross section and differential elastic scattering cross section in the lower energy domain.

In GM model, scattering amplitude is defined as the phase shift function and is extended in the series, where it describes the different multiple scattering processes. The GM model is a semiclassical model picturing the nuclei moving along in the collision direction and it gives a nucleus-nucleus collision in terms of nucleon-nucleon (NN) interaction with the given density distribution. At high energies, this model provides good approximation and, in low energies, the nucleus deflected from the straight-line path due to the Coulomb repulsion. This approach is called the Coulomb modified Glauber model (CMGM) [2, 3]. Many workers have applied CMGM in theory and experiment and successfully calculated the total nuclear reaction cross sections. These calculated values are found to be in good agreement with the experimental results [1, 21].

In the present work, we have calculated the total nuclear reaction cross section for the collision of various projectiles, by using Coulomb modified Glauber model such as $^{56}Fe_{26}$, $^{84}Kr_{36}$, $^{132}Xe_{54}$, $^{197}Au_{79}$, and $^{238}U_{92}$ with different composition elements of the nuclear emulsion nuclei at incident energies $E_{\text{lab}} \sim 1$ GeV/n. In this model, for the reaction calculation, we consider the nuclear medium effect, because, in the medium, nucleon-nucleon (NN) interactions are in some cases different from the free space nucleon-nucleon interactions due to the effects of Pauli blacking and finite nuclear matter density [18]. The calculated total nuclear reaction cross section values are compared with the corresponding projectiles experimental values. From the elements of the nuclear emulsion, we consider the two different chemical compositions according to the emulsion plates company NIKFI (BR-2) and ILFORD (G5) types.

Since, according to the simple geometrical consideration, the total number of projectile participants (P_{proj}), target participants (P_{targ}), and binary collisions (B_c) is calculated [22]. The participant's nucleons and binary collision involved in the collision lead to the calculation of nuclear matter effects. According to the Adamovich [23–27] empirical formula, one can easily calculate the average number of shower particles ($\langle N_S \rangle$) value using the total number of participants and binary collision. Here we have calculated the average number of shower particles value and compared them with corresponding experimental results. We also studied and described the mean free path and nuclear reaction cross section with the projectile mass number.

2. Coulomb Modified Glauber Model

According to the optical limit of the Glauber theory the total nuclear reaction cross section for nucleus-nucleus collision can be written as [2]

$$\sigma_R\,(mb) = 2\pi \int [1 - T\,(b)]\, b \cdot db, \tag{1}$$

where $T(b)$ is the transparency function defined as the probability that a high-energy projectile with the impact parameter b passes through the target without any interaction. The transparency function $T(b)$ is calculated from the projectile and target overlap region, where interactions assumed to be single nucleon-nucleon interaction [2] and it is given by

$$T\,(b) = \exp\left[-\chi\,(b)\right], \tag{2}$$

where the imaginary part of the thickness function or nuclear phase shift function $\chi(b)$, in the case of nucleus-nucleus (A-A) interaction, is given by [2, 3]

$$\chi_{TP}\,(b) = \frac{\overline{\sigma_{NN}}}{10} \int d^2b_P \int_{-\infty}^{\infty} dz_P \int d^2b_T \int_{-\infty}^{\infty} dz_T \rho_P\,(b_P, z_P)\, \rho_T\,(b_T, z_T)\, f\,(b_T - (b - b_P)). \tag{3}$$

And in the case of nucleon-nucleus (h-A) interaction is written as

$$\chi_T\,(b) = \frac{\overline{\sigma_{NN}}}{10} \int d^2b_T \int_{-\infty}^{\infty} dz_T \rho_T\,(b_T, z_T)\, f\,(b_T - b), \tag{4}$$

where $\overline{\sigma_{NN}}$ is the average energy dependent free space nucleon-nucleon (NN) cross section and it is taken from the average of σ_{nn} and σ_{np}. ρ_P and ρ_T are defined as the nuclear density of the projectile and target nuclei. The function

(f) is the finite range of the nucleon-nucleon interaction [3]. The nucleon-nucleon (NN) interaction cross section at intermediate and low energies is modified with medium effect due to the Pauli blocking. The effect of Pauli blocking came from the exclusion principle and it is very essential for the internal region of internuclear distances owing to the high-density overlap region on the colliding nuclei. Therefore, the medium nucleon-nucleon $[(\sigma^{-})^{m}_{NN}]$ cross section is different from the free space nucleon-nucleon interaction cross section $\overline{\sigma_{NN}}$ [18]. In the present work, calculation is also carried out without medium effect:

$$\overline{\sigma_{NN}} = \frac{\left(z_P z_T + N_P N_T\right)\sigma_{pp} + \left(z_P N_T + z_T N_P\right)\sigma_{np}}{A_P A_T}, \quad (5)$$

where A_P, A_T, z_P, z_T, N_P, and N_T are respective projectile and target mass, charge, and neutron numbers. The nucleon-nucleon interaction cross section is from [3, 18]

$$\begin{aligned}\sigma_{nn} &= \sigma_{pp} \\ &= \left(13.73 - 15.04\beta^{-1} + 8.76\beta^{-2} + 68.67\beta^{4}\right) \\ &\quad \times \frac{1.0 + 7.772E_{\text{lab}}^{0.06}\rho^{1.48}}{1.0 + 18.01\rho^{1.46}},\end{aligned} \quad (6)$$

$$\begin{aligned}\sigma_{np} &= \left(-70.67 - 18.18\beta^{-1} + 25.26\beta^{-2} + 113.85\beta\right) \\ &\quad \times \frac{1.0 + 20.88E_{\text{lab}}^{0.04}\rho^{2.02}}{1.0 + 35.86\rho^{1.90}},\end{aligned} \quad (7)$$

where σ_{pp}, σ_{nn}, and σ_{np} is the proton-proton, neutron-neutron, and neutron-proton interaction cross section and it is expressed in millibarn (mb), $\beta = v/c$, E_{lab} is the incident kinetic energy of the nucleon in MeV in the laboratory frame of reference, and ρ is the nuclear matter density in unit of fm^{-3}. In (6) and (7), the first part describes the free space nucleon interaction and the second part describes the nuclear matter effects in the medium nucleon-nucleon interaction cross section. The parameter β is given as [18]

$$\beta = \frac{v}{c} = \sqrt{1.0 - \left(\frac{931.5}{E_{\text{lab}}/A_P + 931.5}\right)^{2}}. \quad (8)$$

Expression (7) is used for the energy $E_{\text{lab}} > 10$ MeV and for energy, $E_{\text{lab}} < 10$ MeV, we have to use another expression as given in the following [3, 28]:

$$\begin{aligned}\sigma_{np} &= \left[\frac{2.73}{\left(1 - 0.0553E_n\right)^{2} + 0.35E_n}\right] \\ &\quad + \left[\frac{17.63}{\left(1 + 0.344E_n\right)^{2} + 6.8E_n}\right].\end{aligned} \quad (9)$$

The projectile and target nuclear matter density distribution is assumed Gaussian in shape as given by [29, 30]

$$\rho_i\left(r_i\right) = \rho_i\left(0\right)\exp\left[\frac{-\left(b_i^2 + z_i^2\right)}{a_i^2}\right], \quad (10)$$

where $i = (P, T)$; a_i and $\rho_i(0)$ are the diffuseness and central nuclear density, respectively. Both of these are related to the root-mean-square radius $[(R)]^{(i)}_{\text{rms}}$, through the following expressions [29, 30]:

$$\begin{aligned}\rho_i\left(0\right) &= \left[\frac{A_i}{\left(a_i\sqrt{\pi}\right)^{3}}\right], \\ a_i &= \sqrt{\frac{2}{3}R^{(i)}_{\text{rms}}},\end{aligned} \quad (11)$$

where $i = P, T$ indicate projectile (P) and target (T). We used the Gaussian form function for the nucleon-nucleon range function [2]:

$$f\left(b\right) = \frac{1}{\pi r_0^2}\exp\left(-\frac{b^2}{r_0^2}\right). \quad (12)$$

Here r_0 parameter is related to the slope of the nucleon-nucleon differential scattering cross section. Integrate (3) with respect to z_P, z_T, b_T, and b_P; the phase shift function $\chi(b)$, for nucleon-nucleus (h-A) interaction is given as [1–3, 31]

$$\chi_T\left(b\right) = \frac{\sqrt{\pi}\rho_T\left(0\right)a_T^3}{10\left(a_T^2 + r_0^2\right)}\overline{\sigma}_{NN}\exp\left(-\frac{b^2}{a_T^2 + r_0^2}\right). \quad (13)$$

While the nucleus-nucleus (A-A) interactions will be obtained by

$$\chi_{PT}\left(b\right) = \chi_{0PT}\exp\left(-\frac{b^2}{a_P^2 + a_T^2 + r_0^2}\right), \quad (14)$$

where

$$\chi_{0PT} = \frac{\pi^2\rho_P\left(0\right)\rho_T\left(0\right)a_P^3 a_T^3}{10\left(a_P^2 + a_T^2 + r_0^2\right)}\overline{\sigma}_{NN}. \quad (15)$$

According to the Coulomb modified Glauber model (CMGM), introducing the effect of Coulomb field between the projectile and target, there is a deviation in the original trajectory of the scattered particle. Therefore, the impact parameter b is replaced by b', which relate the closest approach distance between the interacting particles [3]:

$$b' = \frac{\eta + \sqrt{\left(\eta^2 + k^2b^2\right)}}{k}, \quad (16)$$

where k is a wave number and η is the dimensionless Sommerfeld parameter defined as

$$\eta = \frac{z_P z_T e^2}{\hbar v}, \quad (17)$$

where $z_P e$, $z_T e$ are the total charge of the projectile and target nucleus, respectively, and v is the velocity of the projectile in unit of c. It should be mentioned that, in all our calculations, the overlap integral of (3) and (4) is evaluated in terms of b'. On substituting (14) into (2), one can calculate the total nuclear reaction cross section (σ_R) for the proton and for the

different projectiles interactions with different targets, that is, constituents of nuclear emulsion detector. These calculated nuclear reaction cross sections are used in the calculation of average number of projectile participants $[(P)_{\text{proj}}]$, target participants $[(P)_{\text{targ}}]$, and binary collision $[(B)_C]$ through the following simple geometrical consideration [22]:

$$\left\langle P_{\text{proj}} \right\rangle = \frac{A_P \sigma_{PA_T}}{\sigma_{A_P A_T}},$$
$$\left\langle P_{\text{targ}} \right\rangle = \frac{A_P \sigma_{PA_P}}{\sigma_{A_P A_T}}, \tag{18}$$
$$\left\langle B_C \right\rangle = \frac{A_P A_T \sigma_{nn}}{\sigma_{A_P A_T}}.$$

In the above equations, σ_{PA_T} is the total nuclear reaction cross section of the proton with target, that is, each target belongs to the nuclear emulsion detector constituent; consider, as a target, σ_{PA_P} and σ_{nn} are the total nuclear reaction cross section of the proton with projectile and proton-proton cross section. In addition, $\sigma_{A_P A_T}$ is the total nuclear reaction cross section of the projectile. The average numbers of projectile participants $[(P)_{\text{proj}}]$, target participants $[(P)_{\text{targ}}]$, and binary collision $[(B)_C]$ are used in the shower particle multiplicity calculation.

3. Results and Discussions

We have used the approach discussed in Section 2 for the calculation of total nuclear reaction cross section for proton-emulsion (*h*-*A*), ^{56}Fe-Em, ^{84}Kr-Em, ^{132}Xe-Em, ^{197}Au-Em, and ^{238}U-Em at incident engines ~1 GeV per nucleon. These calculations have been performed in the Coulomb modified Glauber model (CMGM) environment using parameters related to the free space nucleon-nucleon interaction ($\overline{\sigma}_{NN}$) and medium nucleon-nucleon interaction $[(\sigma^-)^m_{NN}]$. Taken into consideration the calculation of total nuclear reaction cross section (σ_R) is $\rho = 0$, in the case without nuclear medium effect. In the case with nuclear medium effect, we used $\rho = 0.15\,\text{fm}^{-3}$, $\rho = 0.17\,\text{fm}^{-3}$, and $\rho = 0.19\,\text{fm}^{-3}$, for the calculation of total nuclear reaction cross section. Here, ρ is the saturation density of the normal nuclear matter, which ranges from 0.15 to $0.19\,\text{fm}^{-3}$ [18]. The calculated nuclear reaction cross section with medium effects is represented as σ^m_{R1}, σ^m_{R2}, and σ^m_{R3}. This *NN* interaction used in this calculation is defined as the medium nucleon-nucleon interaction $[(\sigma^-)^m_{NN}]$ and generally most of the previous calculations [21, 32] considered nuclear matter density $\rho = 0.17\,\text{fm}^{-3}$ only, in their $\overline{\sigma}^m_{NN}$ calculation. It is worth mentioning here that we have performed all theoretical calculation of nuclear reaction cross section in accordance with the zero-range approach. These nuclear reaction cross section values are plotted with respect to the mass number of the different target of the nuclear emulsion detector nuclei for different projectiles at incident kinetic energy around 1 GeV per nucleon in Figures 1 and 2.

From Figures 1 and 2, we may see that the total nuclear reaction cross section with and without nuclear medium effect increases with the mass number of target nucleus, in case of all considered projectiles. From these Figures 1 and 2, one can also observe that the nuclear reaction cross sections σ_R, σ^m_{R1}, σ^m_{R2}, and σ^m_{R3} have very close value to each other in case of the target mass number $A_T < 40$. The total nuclear reaction cross sections with medium effect, σ^m_{R1}, σ^m_{R2}, and σ^m_{R3}, have no significant dependence in the mentioned range of the nuclear matter density (ρ). As shown in Figure 1, there are many calculated/theoretical values of nuclear reaction cross section for proton-emulsion (*h*-*A*); however, the nuclear reaction cross sections without medium effect $[(\sigma)_R]$ have always higher values than the nuclear reaction cross section with medium effects. Figure 2 shows the total nuclear reaction cross section of the heavy projectiles-emulsion (*A*-*A*) interactions for different projectiles as a function of the target mass. The nuclear reaction cross section, σ_R, σ^m_{R1}, σ^m_{R2}, and σ^m_{R3} values, for ^{56}Fe-Em and ^{84}Kr-Em values are close to each other; however, the medium effect values for σ^m_{R1}, σ^m_{R2}, and σ^m_{R3} are dominating in case of ^{132}Xe-Em and ^{238}U-Em, and some place shows protrusions and it may be due to the variation in the projectile mass and nuclear matter density. The nuclear reaction cross section of ^{197}Au-Em shows the clear difference of medium effect $(\sigma)_R$ and without medium effect and in that graph the medium effect nuclear reaction cross section $(\sigma)_R$ values are higher than other three values σ^m_{R1}, σ^m_{R2}, and σ^m_{R3}.

The calculated total nuclear reaction cross section with medium and without medium in case of proton-emulsion (*h*-*A*) and ^{56}Fe-Em, ^{84}Kr-Em, ^{132}Xe-Em, ^{197}Au-Em, and ^{238}U-Em at ~1 GeV/n are tabulated in Tables 1 and 2. It is important to note that the calculated nuclear reaction cross section with medium effect σ^m_{R2} is only given in the table because a previous graph shows that σ^m_{R1}, σ^m_{R2}, and σ^m_{R3} values are closer to each other. It should be mentioned that the first column of the table refers to the constituent elements of the nuclear emulsion, while the second and third column are related to the mass number and root-mean-square (rms) radius of the corresponding elements. In the present study, the rms charge radius is not available for the three projectile nuclei, ^{56}Fe, ^{132}Xe, and ^{197}Au, and it has been calculated using the following global expression [15]:

$$R_{\text{rms}} = 0.891 A^{-1/3}\left(1 + 1.565 A^{-2/3} - 1.04 A^{-4/3}\right). \tag{19}$$

The fifth column referred to the chemical concentration of the element nuclei, NIKFI (Br-2) type of emulsion used for ^{56}Fe-Em, and ^{84}Kr-Em and ILFORD (G5) type of emulsion used in the case of ^{132}Xe-Em, ^{197}Au-Em, and ^{238}U-Em. The sixth and seventh column referred to the calculated total nuclear reaction cross section without medium (σ_R) and with medium effect (σ^m_{R2}) for interaction of proton-emulsion (*h*-*A*) and different projectiles with the emulsion. The multiplied total nuclear reaction cross sections $\sigma^{(ml)}_R$ and $\sigma^{m(ml)}_R$ were obtained from the calculated total nuclear reaction cross sections σ_R and σ^m_{R2} for the different projectiles multiplied with individual emulsion nuclei's (^{1}H, ^{12}C, ^{14}N, ^{16}O, ^{32}S, ^{80}Br, ^{108}Ag, and ^{127}I) chemical concentration. The summation value of $\sigma^{(ml)}_R$ and $\sigma^{m(ml)}_R$ is divided by the sum of the chemical concentration of the elements of the emulsion; one can get the

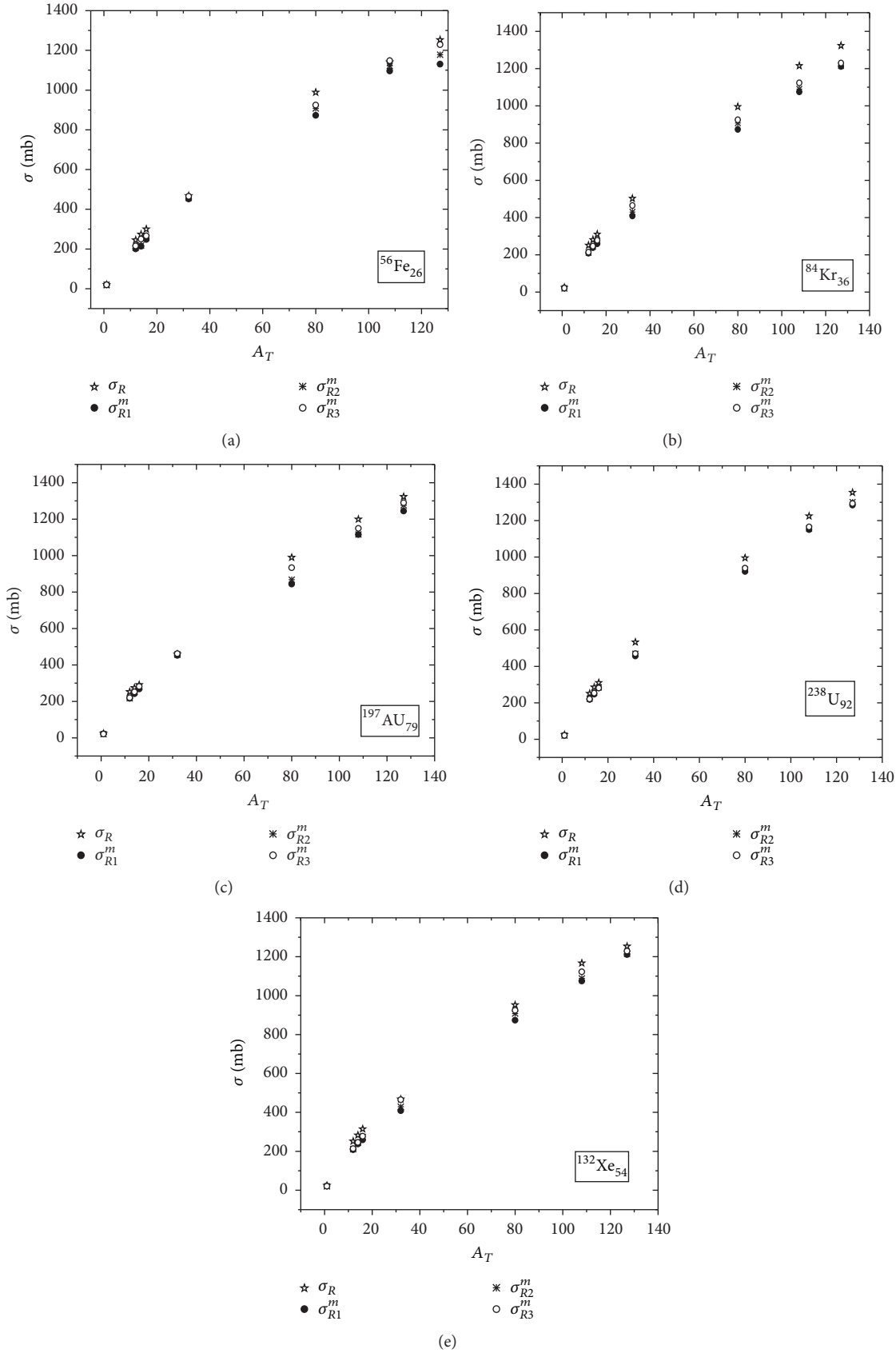

FIGURE 1: The total nuclear reactions cross section of the proton-emulsion (h-A) with medium and without medium effect for the different projectiles as function of emulsion target mass (A_T) are shown from (a) to (e).

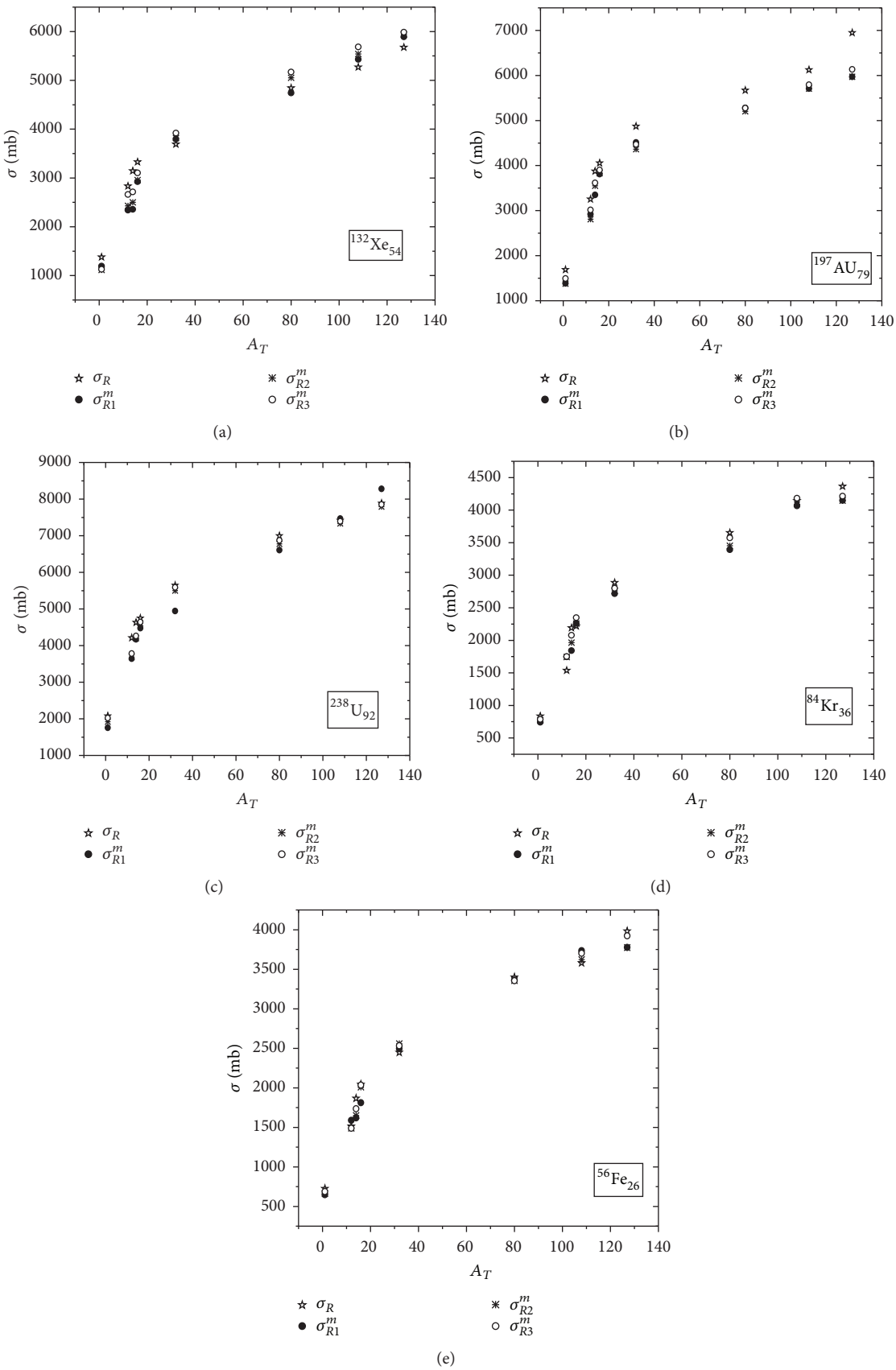

FIGURE 2: The total nuclear reactions cross section of the projectile-emulsion (*A*-*A*) with medium and without medium effect for the different projectiles as function of emulsion target mass (A_T) are shown from (a) to (e).

Table 1: The calculated total nuclear reactions cross-section without nuclear medium effect and with nuclear medium effect in the case of proton-emulsion (*h-A*) interactions for different projectiles at ~1 GeV/n is given below.

Chemical symbol	Mass number	rms radius (fm)	Ref.	Number of atoms (10^{22} cm^{-3})	Without medium effect σ_R (mb)	With medium effect $\sigma^m{}_{R2}$ (mb)	$\sigma^{(ml)}{}_R$ (mb)	$\sigma^{m(ml)}{}_{R2}$ (mb)
				^{56}Fe-Em				
H	1	0.810	[13]	2.93	19.90	19.46	58.33	57.01
C	12	2.442	[2]	1.39	244.93	205.97	340.45	286.29
N	14	2.580	[14]	0.37	273.54	217.5	101.21	80.47
O	16	2.710	[2]	1.06	299.33	256.28	317.29	271.65
S	32	3.251	[2]	0.004	467.13	457.29	1.86	1.82
Br	80	4.151	[15]	1.02	988.27	907.75	1008.03	925.90
Ag	108	4.542	[2]	1.02	1140.55	1122.37	1163.36	1144.81
I	127	4.749	[15]	0.003	1252.63	1178.33	3.75	3.53
				^{84}Kr-Em				
H	1	0.810		2.93	23.51	19.48	68.88	57.07
C	12	2.442		1.39	250.26	211.51	347.86	293.99
N	14	2.580		0.37	280.23	243.85	103.68	90.22
O	16	2.710		1.06	309.47	273.92	328.04	290.35
S	32	3.251		0.004	501.83	429.16	2.00	1.71
Br	80	4.151		1.02	993.94	907.98	1013.82	926.13
Ag	108	4.542		1.02	1214.62	1089.16	1238.91	1110.94
I	127	4.749		0.003	1322.8	1215.31	3.96	3.64
				^{132}Xe-Em				
H	1	0.810		3.251	23.47	20.22	76.32	65.73
C	12	2.442		1.39	251.07	212.86	348.99	295.87
N	14	2.580		0.32	282.2	242.89	90.30	77.72
O	16	2.710		0.94	314.26	278.93	295.40	262.19
S	32	3.251		0.01	467.13	440.76	4.67	4.40
Br	80	4.151		1.01	951.98	910.44	961.49	919.54
Ag	108	4.542		1.02	1166.6	1126.6	1189.93	1149.13
I	127	4.749		0.006	1253.04	1271.7	7.51	7.63
				^{197}Au-Em				
H	1	0.810		3.251	23.45	20.48	76.24	66.58
C	12	2.442		1.39	252.03	217.23	350.32	301.94
N	14	2.580		0.32	273.54	251.86	87.53	80.59
O	16	2.710		0.94	290.10	280.03	272.69	263.22
S	32	3.251		0.01	458.10	457.29	4.58	4.57
Br	80	4.151		1.01	988.66	867.5	998.55	876.17
Ag	108	4.542		1.02	1198.87	1115.45	1222.84	1137.75
I	127	4.749		0.006	1323.06	1275.43	7.93	7.65
				^{238}U-Em				
H	1	0.810		3.251	23.91	20.63	77.73	67.06
C	12	2.442		1.39	250.26	222.11	347.86	308.73
N	14	2.580		0.32	284.80	254.23	91.13	81.35
O	16	2.710		0.94	309.47	283.87	290.90	266.83
S	32	3.251		0.01	532.65	468.17	5.32	4.68
Br	80	4.151		1.01	994.21	930.91	1004.15	940.21
Ag	108	4.542		1.02	1224.28	1155.75	1248.76	1178.86
I	127	4.749		0.006	1353.01	1301.13	8.11	7.80

Table 2: The calculated total nuclear reactions cross-section without medium effect and with nuclear medium effect in case of projectile-emulsion (A-A) interactions for different projectiles at ~1 GeV/n is given below.

Chemical symbol	Mass number	rms radius (fm)	Ref.	Number of atoms (10^{22} cm^{-3})	Without medium effect σ_R (mb)	With medium effect $\sigma_{R2}{}^{m}$ (mb)	$\sigma_R{}^{(ml)}$ (mb)	$\sigma_{R2}{}^{m(ml)}$ (mb)
				^{56}Fe-Em				
H	1	0.810	[13]	2.93	724.14	661.83	2121.75	1939.16
C	12	2.442	[2]	1.39	1511.26	1490.72	2100.65	2072.10
N	14	2.580	[14]	0.37	1865.27	1648.82	690.14	610.06
O	16	2.710	[2]	1.06	2041.85	2010.7	2164.36	2131.34
S	32	3.251	[2]	0.004	2445.98	2558.86	9.78	10.23
Br	80	4.151	[15]	1.02	3398.53	3357.72	3466.50	3424.87
Ag	108	4.542	[2]	1.02	3580.34	3620.3	3651.94	3692.70
I	127	4.749	[15]	0.003	3981.55	3774.63	11.94	11.32
				^{84}Kr-Em				
H	1	0.810		2.93	834.48	773.568	2445.02	2266.55
C	12	2.442		1.39	1537.68	1743.98	2137.37	2424.13
N	14	2.580		0.37	2189.92	1965.44	810.27	727.21
O	16	2.710		1.06	2218.58	2257.47	2351.69	2392.91
S	32	3.251		0.004	2885.14	2759.37	11.54	11.03
Br	80	4.151		1.02	3651.26	3452.15	3724.28	3521.19
Ag	108	4.542		1.02	4142.35	4127.27	4225.19	4209.81
I	127	4.749		0.003	4365.48	4146.67	13.09	12.44
				^{132}Xe-Em				
H	1	0.810		3.251	1378.32	1116.52	4480.91	3629.80
C	12	2.442		1.39	2830.91	2429.46	3934.96	3376.94
N	14	2.580		0.32	3143.44	2500.9	1005.90	800.28
O	16	2.710		0.94	3326.98	2955.95	3127.36	2778.59
S	32	3.251		0.01	3690.55	3818.11	36.90	38.18
Br	80	4.151		1.01	4841.47	5052.64	4889.88	5103.16
Ag	108	4.542		1.02	5269.82	5539.67	5375.21	5650.46
I	127	4.749		0.006	5675.24	5939.52	34.05	35.63
				^{197}Au-Em				
H	1	0.810		3.251	1687.89	1380.52	5487.33	4488.07
C	12	2.442		1.39	3254.06	2810.75	4523.14	3906.94
N	14	2.580		0.32	3874.18	3552.23	1239.73	1136.71
O	16	2.710		0.94	4055.61	3831.86	3812.27	3601.94
S	32	3.251		0.01	4871.57	4365.15	48.71	43.65
Br	80	4.151		1.01	5668.62	5203.02	5725.30	5255.05
Ag	108	4.542		1.02	6125.13	5709.78	6247.63	5823.97
I	127	4.749		0.006	6945.37	5969.96	41.67	35.81
				^{238}U-Em				
H	1	0.810		3.251	2075.47	1923.58	6747.35	6253.55
C	12	2.442		1.39	4208.42	3687.58	5849.70	5125.73
N	14	2.580		0.32	4629.96	4199.16	1481.58	1343.73
O	16	2.710		0.94	4747.73	4607.68	4462.86	4331.21
S	32	3.251		0.01	5641.93	5500.35	56.41	55.00
Br	80	4.151		1.01	6994.17	6777.82	7064.11	6845.59
Ag	108	4.542		1.02	7413.16	7334.71	7561.42	7481.40
I	127	4.749		0.006	7883.63	7795.32	47.30	46.77

average value of the total reaction cross section of the proton-emulsion (h-A) and different projectiles with emulsion (^{56}Fe-Em, ^{84}Kr-Em, ^{131}Xe-Em, ^{197}Au-Em, and ^{238}U-Em) for the complete sample. This calculated average value of the total nuclear reaction cross section has been compared with corresponding experimental data. It should be noted that the experimental total nuclear reaction cross section has been obtained from the following expression [33]:

$$\sigma_R^{\exp} = \frac{1}{n_{cc}\lambda_{\exp}}, \tag{20}$$

where $\lambda_{\exp}$ is the mean free path of the experimental value and n_{cc} is the summation value of the chemical concentration of the elements of emulsion. The experimental mean free path value is playing an important role in the calculation of total nuclear reaction cross section.

In Figure 3, we have plotted the interaction mean free path of different projectiles (^{16}O, ^{40}Ar, ^{12}C, ^{14}C, ^{24}Mg, ^{28}Si, ^{32}S, ^{7}Li, ^{56}Fe, ^{84}Kr, ^{132}Xe, ^{197}Au, and ^{238}U) as a function of the projectile mass number. It is important to note that here all plotted projectiles have different incident energy except for projectiles ^{56}Fe, ^{84}Kr, ^{132}Xe, ^{197}Au, and ^{238}U and the mean free path taken for these projectiles is from [1, 16, 30, 34–38]. Figure 3(a) includes the mean free path (mfp) of ^{197}Au projectile and Figure 3(b) excluded the mfp of ^{197}Au projectile, because the ^{197}Au projectile is only showing the different anomalous effect compared with other projectiles. It is evident from Figure 3 that the mean free path gradually decreases with increasing the projectile mass number. These results indicate that the mean free path strongly depends on the projectile mass number and have weak dependency on the projectile energy.

The calculated projectile-emulsion average value of total nuclear reaction cross section considered with and without nuclear medium effect compared with the corresponding experimental results for different projectiles such as $^{56}Fe_{26}$, $^{84}Kr_{36}$, $^{132}Xe_{54}$, $^{197}Au_{79}$, and $^{238}U_{92}$ at ~1 GeV/n is shown in Figures 4(a) and 4(b). In Figures 4(a) and 4(b), the solid circles represent the experimental reaction cross section for the above-mentioned projectiles. The calculated average value of the nuclear reaction cross section without considering the nuclear medium effect is presented in Figure 4(a) and it is represented as σ_R^{theory}. These calculations have been done using nuclear matter density $\rho = 0$. The average value of nuclear reaction cross section considered with nuclear medium effect is displayed in Figure 4(b). These calculations have been done considering nuclear matter density $\rho = 0.15\,\text{fm}^{-3}$, $\rho = 0.17\,\text{fm}^{-3}$, and $\rho = 0.19\,\text{fm}^{-3}$ and it is represented as $\sigma_{R1}^{(m)\text{theory}}$, $\sigma_{R2}^{(m)\text{theory}}$, and $\sigma_{R3}^{(m)\text{theory}}$. As shown in Figures 4(a) and 4(b), the average value of nuclear reaction cross section continually increases with increasing projectile mass and the calculated theoretical values are always higher than the experimental one. From Figure 4(a), one can observe that the calculated value σ_R^{theory} shows reasonable agreement with corresponding experimental values for projectiles ^{56}Fe-Em, ^{84}Kr-Em, and ^{132}Xe-Em, and it shows disagreement for the projectiles ^{197}Au-Em and ^{238}U-Em. From Figure 4(b), the calculated nuclear reaction cross sections $\sigma_{R1}^{(m)\text{theory}}$, $\sigma_{R2}^{(m)\text{theory}}$, and $\sigma_{R3}^{(m)\text{theory}}$ are closer to each other, and from this figure the average value of nuclear reaction cross section increases with increasing nuclear matter density. The experimental values are in good agreement with the calculated ones for the projectiles ^{56}Fe-Em, ^{84}Kr-Em, and ^{132}Xe-Em and disagreement for the projectiles ^{197}Au-Em and ^{238}U-Em.

From these graphs (Figures 4(a) and 4(b)), one can observe that the ^{197}Au projectile experimental nuclear reaction cross section and predicted nuclear reaction cross section show large difference. It is due to the experimental nuclear reaction cross section value highly suppressed for the ^{197}Au projectile. The reason behind this is unknown. The experimental nuclear reaction cross section value has been calculated using the mean free path (λ) value of ^{197}Au projectile [17]. From Figure 4(b), we can conclude that the calculated nuclear reaction cross section with medium effect shows good agreement with experimental values within the statistical error except for ^{197}Au. The ^{197}Au projectile only shows the anomalous effect compared to the other projectiles, so it is very important to recheck the ^{197}Au projectile experimental mean free path value. From the above results, we may conclude that introducing the nuclear medium effect is necessary for the Coulomb modified Glauber model for the descriptions of heavy-ion collision. We may also conclude that the nuclear reaction cross sections with medium effect have lower value than the without medium effect. These changes may occur by decreases of nucleon-nucleon (NN) interaction cross section due to the consideration of nuclear medium. The calculation of nuclear reaction cross section not only depends on the radii of projectile and target but also depends on the projectile mass and medium.

In Figure 5, the energy dependence of the average value of the total nuclear reaction cross sections is shown. It shows that the calculated average value of the total nuclear reaction cross section [σ_R^{theory}] without nuclear medium effect for projectiles $^{56}Fe_{26}$, $^{84}Kr_{36}$, $^{132}Xe_{54}$, $^{197}Au_{79}$, and $^{238}U_{92}$ at ~1 GeV/n are compared with $^{16}O_{32}$ projectile of different energy from 0.2 GeV to 200 GeV. The calculated and experimental values for $^{16}O_{32}$ projectile are taken from [1]. It can be seen from Figure 5 that the calculated nuclear reaction cross section for ^{16}O-Em at 0.2 GeV/n and ^{56}Fe-Em, ^{84}Kr-Em, and ^{132}Xe-Em at ~1 GeV/n is showing reasonable agreement with the experimental values. The ^{16}O-Em interactions above 2 GeV show significant disagreement with the experimental results and they also show disagreement with the higher-mass projectiles such as ^{197}Au-Em and ^{238}U-Em. It is reflected that the present model is not suitable for the higher-mass and higher-energy projectiles and further modification should be considered.

In Figure 6, we displayed the ratio of $\sigma_{\text{Expt}}/\sigma_{\text{Cal}}$ as the function of projectile mass for $^{56}Fe_{26}$, $^{84}Kr_{36}$, $^{132}Xe_{54}$, $^{197}Au_{79}$, and $^{238}U_{92}$ at ~1 GeV/n. From Figure 6, one can see that the model predicted value of the nuclear reaction cross section is close to the experimentally measured nuclear reaction cross section value for the projectiles $^{56}Fe_{26}$, $^{84}Kr_{36}$ and $^{132}Xe_{54}$. However, it fails to predict the same for the projectiles $^{197}Au_{79}$

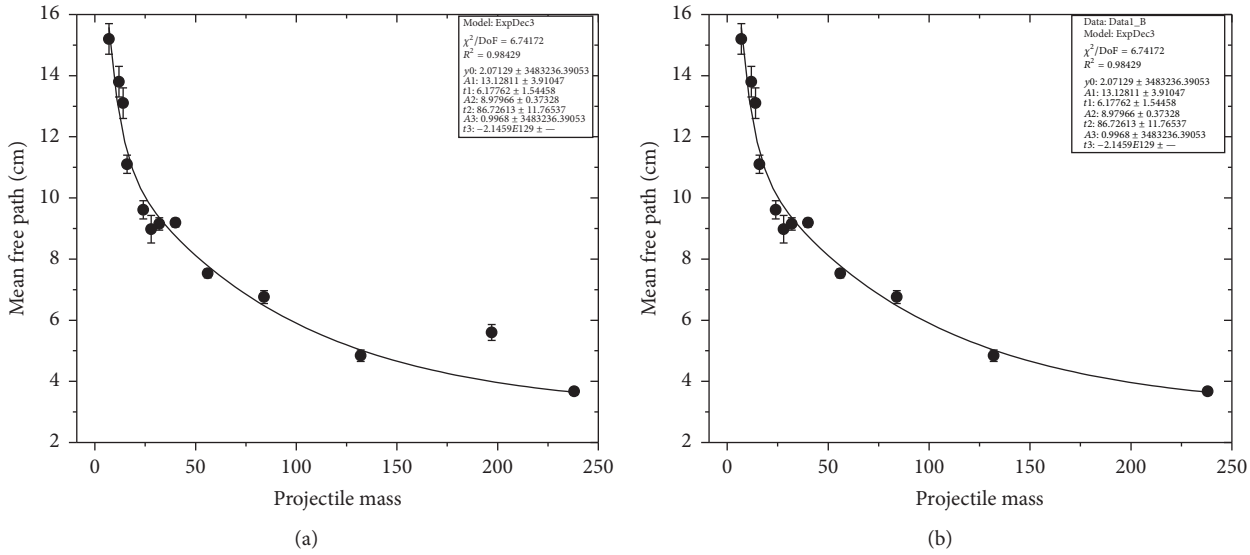

FIGURE 3: (a) The experimental mean free path of different projectiles as a function of a projectile mass number (b) without $^{197}Au_{79}$ projectile data.

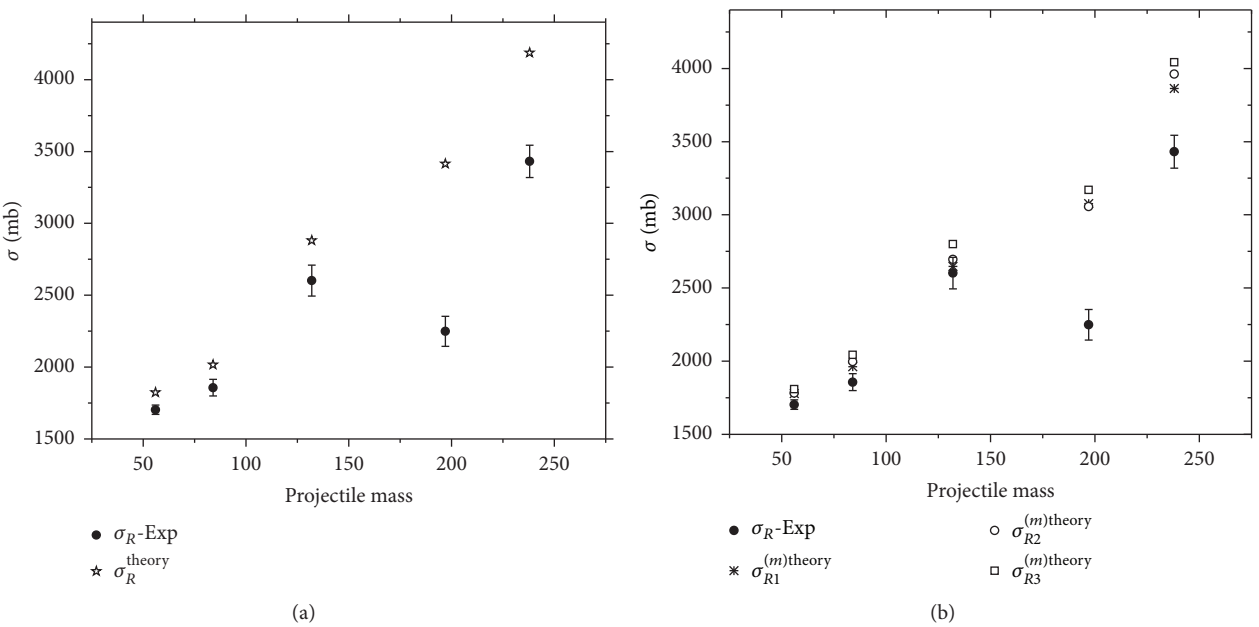

FIGURE 4: (a) The average value of total reaction cross section considered without medium effect. (b) The average value of total reaction cross section considered with medium effect and both are corresponding to the experimental data for different projectiles $^{56}Fe_{26}$, $^{84}Kr_{36}$, $^{132}Xe_{54}$, $^{197}Au_{79}$, and $^{238}U_{92}$ at ~1 GeV/n.

and $^{238}U_{92}$. It is shown that the proposed model needs further modification to explain the similar phenomena for heavy nuclei such as $^{197}Au_{79}$ and $^{238}U_{92}$.

Using the CMGM approaches, we have also calculated the average number of projectile participants (P_{proj}), target participants (P_{targ}), and binary collision (B_C) over the different constituents of nuclear emulsion detector for the interaction of different projectiles. The obtained values are tabulated in Tables 3 and 4. For the calculation of the above-mentioned parameters, we used (18). In these equations, nucleus-nucleus $\sigma_{(A_PA_T)}$, proton-nucleus $\sigma_{(P_PP_T)}$, and proton-proton $\sigma_{(PP)}$ cross section are parameterized as [33]

$$\begin{aligned}
\sigma_{(A_PA_T)}\ (\text{mb}) &= 109.2\left(A_P{}^{0.29} + A_T{}^{0.29} - 1.39\right)^2, \\
\sigma_{(P_PP_T)}\ (\text{mb}) &= 38.17A^{0.719}, \\
\sigma_{(PP)}\ (\text{mb}) &= 32.3\ (\text{mb}).
\end{aligned} \tag{21}$$

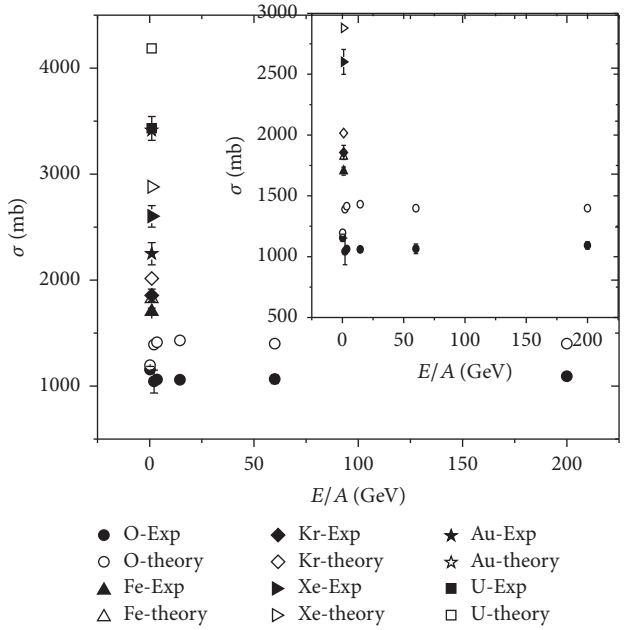

Figure 5: Energy dependence of the nuclear reaction cross section for the $^{56}Fe_{26}$, $^{84}Kr_{36}$, $^{132}Xe_{54}$, $^{197}Au_{79}$, $^{238}U_{92}$, and $^{16}O_8$ projectiles. Inset plot is the zoomed one.

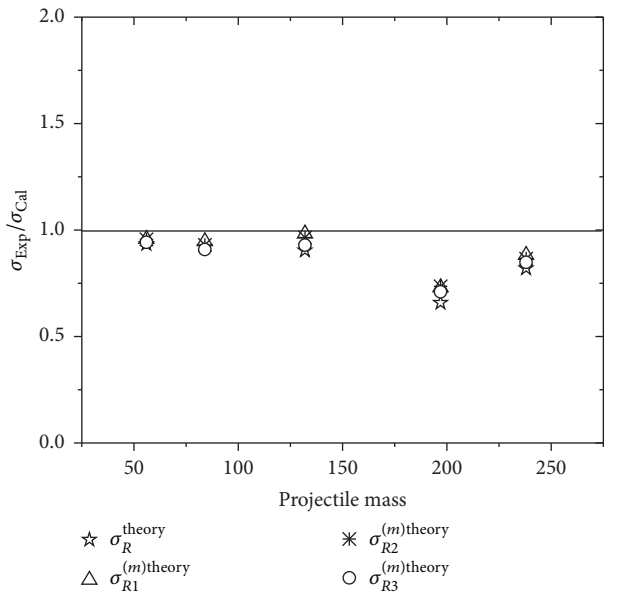

Figure 6: Ratio of $\sigma_{exp}/\sigma_{cal}$ as the function of projectile mass for $^{56}Fe_{26}$, $^{84}Kr_{36}$, $^{132}Xe_{54}$, $^{197}Au_{79}$, and $^{238}U_{92}$ at incident energies ~ 1 GeV/n.

From Tables 3 and 4, one can see that the values of projectile participants, target participants, and binary collision for the interactions of any considered projectiles with the corresponding nuclear emulsion detector's target nuclei increase as the mass number of the target nuclei is increasing. From Table 3, one can observe that the projectile participant has unit value for the interaction of proton with the nuclear emulsion detector's nucleus except in the case of hydrogen target nucleus. On the other hand, the value of projectile participants and target participants, for the interaction of proton with H-nucleus, is the same for the projectiles $^{56}Fe_{26}$, $^{84}Kr_{36}$, $^{132}Xe_{54}$, $^{197}Au_{79}$, and $^{238}U_{92}$. In the case of proton-Em, the summed values of P_{proj} and P_{targ} in the reactions ^{56}Fe-^{1}H, ^{84}Kr-^{1}H, ^{132}Xe-^{1}H, ^{197}Au-^{12}C, and ^{238}U-^{1}H or ^{56}Fe-^{12}C, Kr-^{12}C, ^{132}Xe-^{12}C, ^{197}Au-^{12}C, ^{238}U-^{12}C, and so on are usually higher than the values of the binary collisions. The values of target participants and binary collision, in the case of nuclear medium effects and proton-proton collision for the interaction of various projectiles with the same target nucleus of the nuclear emulsion detector (such as ^{56}Fe-^{12}C, ^{84}Kr-^{12}C, ^{132}Xe-^{12}C, ^{197}Au-^{12}C, and ^{238}U-^{12}C), decrease with increase in the mass number of the projectiles. From Table 4, we may see that the same parameters are increasing with the increase in the projectile mass number in case of nucleus-nucleus (*A*-*A*) collisions and keeping the rest of the conditions the same as above, that is, in case of Table 3. From Table 4, it is clear that the calculated total nuclear reaction cross section with and without nuclear medium effects is larger in case of nucleus-nucleus (*A*-*A*) collisions than the values obtained in case of proton-nucleus (*h*-*A*) collision, which are tabulated in Table 3. This may be due the multiple number of collisions among the nucleons of the two colliding nucleus. From Tables 3 and 4, we may conclude that the number of projectile participants, target participants, and the participant from the binary collision are heavily dependent on the mass number of the colliding nuclei that also strongly supports the theory of superposition of nucleon, that is, multiple collisions during nucleus-nucleus interactions.

The calculated number of average projectile participants and target participants and average number of binary collision for different projectile have been tabulated in Table 4. Considering the CMGM model approach and without nuclear matter effects, the average number of participants, that is, the sum of projectile and target participants, is 27.39 and 37.56 and the number of binary collisions is obtained for the case of $^{84}Kr_{36}$-Em interactions at around 1 GeV per nucleon kinetic energy. In the case of proton-proton collision, the same parameters for $^{84}Kr_{36}$-Em interactions are 3.56 and 2.10, respectively. The ratio of nucleus-nucleus and proton-proton collisions for the number of participating nucleons and the number of binary interactions in a collision will shed some light on the growth of the amount of nuclear matter involved in the collision of proton-proton to nucleus-nucleus, and the rations for the $^{84}Kr_{36}$-Em interactions are 7.69 and 17.88, respectively. The estimate of average number of produced pions and kaons in an interaction can be obtained using following equations [35].

For the proton-nucleus/proton collisions,

$$\langle n_s \rangle_{P\text{-Em}} = 2.34 \langle n_s \rangle_{PP} - 4.12. \quad (22)$$

From the nucleus-nucleus collisions,

$$\langle n_s \rangle_{^{84}Kr_{36}\text{-Em}} = 17.99 \langle n_s \rangle_{PP} - 31.68. \quad (23)$$

And for the binary collision approach,

$$\langle n_s \rangle_{^{84}Kr_{36}\text{-Em}} = 41.83 \langle n_s \rangle_{PP} - 73.66. \quad (24)$$

Table 3: Amount of nuclear matter involved in the proton-emulsion (h-A) interaction for different projectiles with nuclear emulsion target at incident energies ~1 GeV/n is estimated. These calculated values are averaged over the impact parameter.

Chemical symbol	Mass number	rms radius (fm)	Without medium effect σ_R (mb)	With in-medium effect $\sigma_{R2}{}^m$ (mb)	Without medium effect			With in-medium effect		
					P_{proj}	P_{targ}	B_C	P_{proj}	P_{targ}	B_C
				^{56}Fe-Em						
H	1	0.810	19.90	19.46	1.91	1.91	1.62	1.96	1.96	1.65
C	12	2.442	244.93	205.97	1	1.87	1.58	1.10	2.22	1.88
N	14	2.580	273.54	217.5	1	1.95	1.65	1.17	2.45	2.07
O	16	2.710	299.33	256.28	1	2.04	1.72	1.09	2.38	2.01
S	32	3.251	467.13	457.29	1	2.61	2.21	1	2.67	2.26
Br	80	4.151	988.27	907.75	1	3.08	2.61	1	3.36	2.84
Ag	108	4.542	1140.55	1122.37	1	3.61	3.05	1	3.67	3.10
I	127	4.749	1252.63	1178.33	1	3.86	3.27	1.05	4.11	3.48
				^{84}Kr-Em						
H	1	0.810	23.51	19.48	1.62	1.62	1.37	1.95	1.95	1.65
C	12	2.442	250.26	211.51	1	1.83	1.54	1.07	2.16	1.83
N	14	2.580	280.23	243.85	1	1.90	1.61	1.04	2.19	1.85
O	16	2.710	309.47	273.92	1	1.97	1.66	1.02	2.22	1.88
S	32	3.251	501.83	429.16	1	2.43	2.05	1.07	2.84	2.40
Br	80	4.151	993.94	907.98	1	3.07	2.59	1	3.36	2.84
Ag	108	4.542	1214.62	1089.16	1	3.39	2.87	1.01	3.78	3.20
I	127	4.749	1322.8	1215.31	1	3.6	3.10	1.02	3.98	3.37
				^{131}Xe-Em						
H	1	0.810	23.47	20.22	1.62	1.62	1.37	1.88	1.88	1.59
C	12	2.442	251.07	212.86	1	1.82	1.54	1.07	2.15	1.82
N	14	2.580	282.2	242.89	1	1.89	1.60	1.04	2.20	1.86
O	16	2.710	314.26	278.93	1	1.94	1.64	1	2.18	1.85
S	32	3.251	467.13	440.76	1	2.61	2.21	1.04	2.77	2.34
Br	80	4.151	951.98	910.44	1	3.20	2.71	1	3.35	2.83
Ag	108	4.542	1166.6	1126.6	1	3.53	2.99	1	3.65	3.09
I	127	4.749	1253.04	1271.7	1	3.86	3.27	1	3.81	3.22
				^{197}Au-Em						
H	1	0.810	23.45	20.48	1.62	1.62	1.37	1.86	1.86	1.57
C	12	2.442	252.03	217.23	1	1.81	1.53	1.04	2.10	1.78
N	14	2.580	273.54	251.86	1	1.95	1.65	1.01	2.12	1.79
O	16	2.710	290.10	280.03	1	2.10	1.78	1	2.18	1.84
S	32	3.251	458.10	457.29	1	2.66	2.25	1	2.67	2.26
Br	80	4.151	988.66	867.5	1	3.08	2.61	1.02	3.52	2.97
Ag	108	4.542	1198.87	1115.45	1	3.43	2.90	1	3.69	3.12
I	127	4.749	1323.06	1275.43	1	3.66	3.10	1	3.80	3.21
				^{238}U-Em						
H	1	0.810	23.91	20.63	1.59	1.59	1.35	1.85	1.85	1.56
C	12	2.442	250.26	222.11	1	1.83	1.54	1.02	2.06	1.74
N	14	2.580	284.80	254.23	1	1.87	1.58	1	2.10	1.77
O	16	2.710	309.47	283.87	1	1.97	1.66	1	2.15	1.82
S	32	3.251	532.65	468.17	1	2.29	1.94	1	2.60	2.20
Br	80	4.151	994.21	930.91	1	3.07	2.59	1	3.28	2.77
Ag	108	4.542	1224.28	1155.75	1	3.36	2.84	1	3.56	3.01
I	127	4.749	1353.01	1301.13	1	3.58	3.03	1	3.72	3.15

Table 4: The amount of nuclear matter involved in the projectile-emulsion (A-A) interaction for different projectiles with nuclear emulsion target at incident energies ~1 GeV/n is estimated. These calculated values are averaged over the impact parameter.

Chemical symbol	Mass number	rms radius (fm)	Without medium effect σ_R (mb)	With medium effect $\sigma_{R2}{}^m$ (mb)	Without medium effect			With medium effect		
					P_{proj}	P_{targ}	B_C	P_{proj}	P_{targ}	B_C
				^{56}Fe-Em						
H	1	0.810	724.14	661.83	2.95	1	2.49	3.22	1.04	2.73
C	12	2.442	1511.26	1490.72	8.44	5.47	14.36	8.55	5.55	14.56
N	14	2.580	1865.27	1648.82	7.64	5.17	13.57	8.64	5.85	15.35
O	16	2.710	2041.85	2010.7	7.68	5.40	14.17	7.80	5.48	14.39
S	32	3.251	2445.98	2558.86	10.55	9.02	23.66	10.09	8.62	22.62
Br	80	4.151	3398.53	3357.72	14.68	16.23	42.57	14.86	16.43	43.09
Ag	108	4.542	3580.34	3620.3	17.29	20.80	54.56	17.10	20.57	53.95
I	127	4.749	3981.55	3774.63	17.47	21.99	57.69	18.43	23.20	60.85
				^{84}Kr-Em						
H	1	0.810	834.48	773.568	3.84	1.10	3.25	4.14	1.19	3.50
C	12	2.442	1537.68	1743.98	12.44	7.20	21.17	10.97	6.35	18.66
N	14	2.580	2189.92	1965.44	9.76	5.90	17.34	10.87	6.57	19.32
O	16	2.710	2218.58	2257.47	10.60	6.65	19.56	10.42	6.54	19.23
S	32	3.251	2885.14	2759.37	13.42	10.23	30.09	14.04	10.70	31.46
Br	80	4.151	3651.26	3452.15	20.50	20.22	59.44	21.68	21.39	62.87
Ag	108	4.542	4142.35	4127.27	22.42	24.06	70.73	22.50	24.15	70.99
I	127	4.749	4365.48	4146.67	23.91	26.85	78.93	25.17	28.27	83.09
				^{131}Xe-Em						
H	1	0.810	1378.32	1116.52	3.65	1	3.09	4.51	1.144	3.81
C	12	2.442	2830.91	2429.46	10.62	5.41	18.07	12.37	6.31	21.05
N	14	2.580	3143.44	2500.9	10.68	5.69	18.98	13.43	7.15	23.86
O	16	2.710	3326.98	2955.95	11.11	6.14	20.50	12.51	6.91	23.07
S	32	3.251	3690.55	3818.11	16.49	11.07	36.96	15.94	10.70	35.73
Br	80	4.151	4841.47	5052.64	24.30	21.11	70.45	23.28	20.22	67.50
Ag	108	4.542	5269.82	5539.67	27.70	26.18	87.37	26.35	24.90	83.12
I	127	4.749	5675.24	5939.52	28.90	28.59	95.41	27.61	27.31	91.16
				^{197}Au-Em						
H	1	0.810	1687.89	1380.52	4.45	1	3.76	5.44	1.23	4.60
C	12	2.442	3254.06	2810.75	13.79	6.28	23.46	15.96	7.27	27.16
N	14	2.580	3874.18	3552.23	12.94	6.15	22.99	14.11	6.71	25.07
O	16	2.710	4055.61	3831.86	13.61	6.72	25.10	14.40	7.11	26.56
S	32	3.251	4871.57	4365.15	18.65	11.19	41.79	20.81	12.49	46.64
Br	80	4.151	5668.62	5203.02	30.97	24.04	89.80	33.74	26.19	97.83
Ag	108	4.542	6125.13	5709.78	35.57	30.04	112.19	38.15	32.22	120.35
I	127	4.749	6945.37	5969.96	35.24	31.15	116.35	41	36.24	135.36
				^{238}U-Em						
H	1	0.810	2075.47	1923.58	4.37	1	3.70	4.72	1.01	3.99
C	12	2.442	4208.42	3687.58	12.88	5.56	21.92	14.70	6.35	25.01
N	14	2.580	4629.96	4199.16	13.08	5.90	23.24	14.42	6.50	25.62
O	16	2.710	4747.73	4607.68	14.04	6.57	25.90	14.47	6.77	26.69
S	32	3.251	5641.93	5500.35	19.45	11.07	43.60	19.95	11.35	44.72
Br	80	4.151	6994.17	6777.82	30.33	22.32	87.92	31.29	23.03	90.73
Ag	108	4.542	7413.16	7334.71	35.50	28.43	111.99	35.88	28.74	113.19
I	127	4.749	7883.63	7795.32	37.51	31.44	123.83	37.94	31.80	125.24

Table 5: The calculated average values of shower particles multiplicities in the framework of CGCM with and without nuclear medium effect approaches compared with corresponding experimental values at ~1 GeV/n.

Reaction systems	$\langle n_s \rangle^{\text{Exp}}$	Ref.	Calculation with nuclear medium effect			Calculation without nuclear medium effect		
			$\langle n_s \rangle$ $(P_{\text{prog}} + P_{\text{targ}})$	$\langle n_s \rangle$ B_C	$\langle n_s \rangle^{\text{theory}}$	$\langle n_s \rangle$ $(P_{\text{prog}} + P_{\text{targ}})$	$\langle n_s \rangle$ B_C	$\langle n_s \rangle^{\text{theory}}$
^{56}Fe-Em	—	—	21.47	27.88	10.26	21.93	28.44	9.64
^{84}Kr-Em	13.14 ± 0.39	[9]	27.39	37.56	14.29	28.11	38.64	13.05
^{132}Xe-Em	17.40 ± 0.70	[16]	29.82	43.85	15.90	30.08	43.66	14.83
^{197}Au-Em	16.43 ± 3.43	[17]	35.23	54.43	19.59	39.13	60.45	20.24
^{238}U-Em	—	—	34.93	55.26	20.48	36.11	56.90	19.49

From (22), one can understand that the average multiplicity of singly charged relativistic particles in the proton-emulsion nucleus interactions ($\langle n_s \rangle_{P\text{-Em}}$) linearly depends on the charged particle multiplicity in the case of proton-proton interaction ($\langle n_s \rangle_{PP}$), at the same energy [23–27]. In addition to the resultant values of (23) and (24), one can get the average multiplicity of singly charged relativistic particles for ^{84}Kr-Em interaction at ~1 GeV/n. Following the above-mentioned procedures, we obtained the value of charged relativistic particles for different reaction ^{56}Fe-Em, ^{132}Xe-Em, ^{197}Au-Em, and ^{238}U-Em. It is worth mentioning here that in a similar fashion we have calculated the value of the relativistic charged particles for medium effect. The calculated average values of the singly charged relativistic particles or shower particle's multiplicities are compared with the corresponding experimental values shown in Table 5.

From Table 5, we may see that the calculated shower particles (i.e., produced particles during collisions) multiplicities from the Coulomb modified Glauber model (CGCM) consideration with and without medium effect successfully reproduce the experimental results within statistical error. Since the calculated participant multiplicity values are less than the binary collision values according to the CGCM calculation, therefore, it indicates that the expected large number of shower particles is mainly coming from the binary collision in case of all reactions. This effect may be seen for both cases with and without nuclear medium effect. We can also observe that the experimental and calculated values of shower particles multiplicities are linearly increasing with increase in the projectiles mass number and incident kinetic energy [1].

4. Conclusions

In this work, we have calculated and compared the total nuclear reaction cross section for proton-emulsion (*h*-*A*) and nucleus-emulsion (*A*-*A*) interactions considering the cases with and without nuclear medium effects for large number of projectiles at the incident kinetic energy of ~1 GeV per nucleon in the framework of Coulomb modified Glauber model (CMGM). For the calculation of nuclear reaction cross section with nuclear medium effect, we considered different values of nuclear matter density. All theoretical calculations presented in this paper are performed in zero-range approach. The small change in nuclear matter density of nucleon-nucleon (*N*-*N*) interaction cross section does not produced any remarkable changes in nucleus-nucleus (*A*-*A*) interactions cross section and in the proton-emulsion (*h*-*A*) interactions cross section. However, comparison results represent that introducing the nuclear medium effect is necessary for the Coulomb modified Glauber model for the descriptions of heavy-ion collision. The total nuclear reaction cross sections are also calculated for the different constituents of the nuclear emulsion detector's nuclei. From the results, it may be concluded that the CMGM model generally described the total reaction cross section on the mean free path of the projectiles considered in emulsion around the 1 GeV per nucleon, except for the heavy incident nuclei. In most of the cases, the average values of projectile-emulsion nuclear reaction cross section are compared with the corresponding experimental results and show significant agreements. We observed that the nuclear reaction cross sections with nuclear medium effect predict less value than the without nuclear medium effect. These changes may be possible due to decrease in the nucleon-nucleon (*N*-*N*) cross section in the presence of nuclear medium. Since the average value of nuclear reaction cross section continuously increases with increase in the projectile mass number, however, we observed that the calculated results without nuclear medium effect are in fairly good agreement with experimental results of projectiles ^{56}Fe, ^{84}Kr, and ^{132}Xe and show disagreement with results of projectiles ^{197}Au and ^{238}U. We observed similar results in case of nuclear medium effect. Since results obtained from CMGM analysis for ^{197}Au projectile only differ strongly with the experimental results, therefore, it is important to pay more attention on the experimental result of the ^{197}Au projectile mean free path. The calculated average value of nuclear reaction cross section without nuclear medium effect has been compared in different energy regions of ^{16}O projectile. Results showed reasonably good agreement with calculated one. It may be an indication that the model should be modified for high mass and energy regions. The experimental mean free path value has strong influence on the experimental nuclear reaction cross section. We observed the same with weak dependence of kinetic energy of the projectile. The ratio of $\sigma_{\text{Expt}}/\sigma_{\text{Cal}}$ as the function of projectile mass graph revealed that the CMGM prediction for the nuclear reaction cross sections is very close to the experimental results for the projectiles ^{56}Fe, ^{84}Kr, and ^{132}Xe. We have also calculated the number of binary collisions

for the proton-emulsion and nucleus-emulsion interactions cross sections considering cases with and without nuclear medium effect. These average values are used in calculation of the average values of the shower particles. The calculated values of shower particles for different projectiles are compared with the corresponding experimental value and found in good agreement. The shower particles multiplicities depend on the projectile mass and as well as incident energy of the projectiles.

Conflicts of Interest

The authors declare that they have no conflicts of interest.

Acknowledgments

The authors are thankful to the Department of Science and Technology (DST), New Delhi, for their financial support.

References

[1] M. S. M. Nour El-Din and M. E. Solite, "A study of the energy dependence for the multiplicity of shower particles produced in a ^{16}O–emulsion interaction in the framework of the Coulomb-modified Glauber model," *Canadian Journal of Physics*, vol. 86, article 1209, 2008.

[2] A. Y. Abul-Magd and M. T. Ali-Alhinai, "The Coulomb-modified Glauber description of reaction cross-sections of heavy ions with nuclei," *Il Nuovo Cimento A* , vol. 110, no. 11, pp. 1281–1288, 1997.

[3] S. K. Charagi and S. K. Gupta, "Coulomb-modified Glauber model description of heavy-ion reaction cross sections," *Physical Review C: Nuclear Physics*, vol. 41, no. 4, pp. 1610–1618, 1990.

[4] J. Chauvin, D. Lebrun, A. Lounis, and M. Buenerd, "Low and intermediate energy nucleus-nucleus elastic scattering and the optical limit of Glauber theory," *Physical Review C*, vol. 28, p. 1970, 1983.

[5] M. Y. H. Farag, "Modified Glauber model for the total reaction cross-section of ^{12}C + ^{12}C collisions," *The European Physical Journal A - Hadrons and Nuclei*, vol. 2, p. 405, 2001.

[6] M. K. Singh, A. K. Soma, R. Pathak, and V. Singh, "Two source emission behavior of projectile fragments alpha in ^{84}Kr interactions at around 1 GeV per nucleon," *Indian Journal of Physics*, vol. 85, no. 10, pp. 1523–1533, 2011.

[7] V. Singh et al., "Multifragmentation Studies in ^{84}Kr Interactions with Nuclear Emulsion at around 1 A GeV".

[8] N. Marimuthu, V. Singh, and S. S. R. Inbanathan, "Characteristics study of projectile's lightest fragment for $^{84}Kr_{36}$–emulsion interaction at around 1 A GeV," *Indian Journal of Physics*, vol. 91, no. 4, pp. 431–438, 2017.

[9] V. Singh, *An Investigation of 84Kr-Emulsion interactions around 1Gev per nucleon - Thesis*, Banaras Hindu University, Varanasi, 1998.

[10] N. S. Chouhan, M. K. Singh, V. Singh, and R. Pathak, "Characteristics of compound multiplicity in 84Kr36 with various light and heavy targets at 1 GeV per nucleon," *Indian Journal of Physics*, vol. 87, no. 12, pp. 1263–1267, 2013.

[11] M. K. Singh, R. Pathak, and V. Singh, "Characteristics of alpha projectile fragments emission in interaction of nuclei with emulsion," *Indian Journal of Physics*, vol. 84, no. 9, pp. 1257–1273, 2010.

[12] M. K. Singh, A. K. Soma, R. Pathak, and V. Singh, "Multiplicity distributions of shower particles and target fragments in $^{84}Kr_{36}$–emulsion interactions at 1 GeV per nucleon," *Indian Journal of Physics*, vol. 88, no. 3, pp. 323–327, 2014.

[13] V. Franco and G. K. Varma, "Collisions between composite particles at medium and high energies," *Physical Review C: Nuclear Physics*, vol. 18, no. 1, pp. 349–370, 1978.

[14] H. De Vries, C. W. De Jager, and C. De Vries, "Nuclear charge-density-distribution parameters from elastic electron scattering," *Atomic Data and Nuclear Data Tables*, vol. 36, no. 3, pp. 495–536, 1987.

[15] J. Friedrich and N. Voegler, "The salient features of charge density distributions of medium and heavy even-even nuclei determined from a systematic analysis of elastic electron scattering form factors," *Nuclear Physics A*, vol. 373, no. 2, pp. 192–224, 1982.

[16] http://www.iaea.org/inis/collection/NCLCollectionStore/_Public/27/006/27006912.pdf.

[17] C. J. Waddington and P. S. Freier, "Interactions of energetic gold nuclei in nuclear emulsions," *Physical Review C*, vol. 31, p. 888, 1985.

[18] C. Xiangzhou et al., "In-medium nucleon-nucleon cross section and its effect on total nuclear reaction cross section," *Physical Review C*, vol. 58, p. 572, 1998.

[19] R. J. Glauber, *Lectures in Theoretical Physics*, W. E. Brittin et al., Ed., vol. 1, Inter Science Publishers, New York, NY, USA, 1959.

[20] R. J. Glauber and G. Matthiae, "High-energy scattering of protons by nuclei," *Nuclear Physics B*, vol. 21, no. 2, pp. 135–157, 1970.

[21] Y. J. Kim, "Coulomb-modified Glauber Model Analysis for ^{6}Li + ^{58}Ni and ^{6}Li + ^{90}Zr Elastic Scatterings at E_{lab} = 600 MeV," *New Physics: Sae Mulli*, vol. 64, no. 4, pp. 389–395, 2014.

[22] M. A. Jilany et al., "Interactions of relativistic ^{24}Mg nuclei with emulsion nuclei at 4.5 GeV/c per nucleon," *International Journal of Modern Physics E*, vol. 4, pp. 815–825, 1995.

[23] M. I. Adamovich, M. M. Aggarwa, Y. A. Alexandrov et al., "Complex analysis of gold interactions with photoemulsion nuclei at 10.7 GeV/nucleon within the framework of cascade and FRITIOF models," *Zeitschrift für Physik A: Hadrons and Nuclei*, vol. 358, no. 3, pp. 337–351, 1997.

[24] M. I. Adamovich, M. M. Aggarwa, Y. A. Alexandrov et al., "Charged particle multiplicity and pseudorapidity density distributions in ^{16}O, ^{28}Si and ^{197}Au-induced nuclear interactions at 14.6 and 11.6*A* GeV/*c*," *Nuclear Physics A*, vol. 593, no. 4, pp. 535–549, 1995.

[25] M. I. Adamovich, M. M. Aggarwa, Y. A. Alexandrov et al., "Charged particle density distributions in Au induced interactions with emulsion nuclei at 10.7 A GeV," *Physics Letters B*, vol. 352, no. 3-4, pp. 472–478, 1995.

[26] M. I. Adamovich, M. M. Aggarwa, Y. A. Alexandrov et al., "Local particle densities and global multiplicities in central heavy ion interactions at 3.7, 14.6, 60 and 200*A* GeV," *Zeitschrift für Physik C Particles and Fields*, vol. 56, no. 4, pp. 509–520, 1992.

[27] M. I. Adamovich, M. M. Aggarwal, and N. P. Andreeva, "Rapidity densities and their fluctuations in central 200 A GeV ^{32}S interactions with Au and Ag, Br nuclei EMU01 collaboration," *Physics Letters B*, vol. 227, p. 285, 1987.

[28] P. Shukla, "Glauber model for heavy ion collisions from low energies to high energies," 2001, https://arxiv.org/abs/nucl-th/0112039.

[29] P. J. Karol, "Nucleus-nucleus reaction cross sections at high energies: Soft-spheres model," *Physical Review C: Nuclear Physics*, vol. 11, no. 4, pp. 1203–1209, 1975.

[30] P. J. Karol, "Transparency in high-energy nuclear collisions," *Physical Review C: Nuclear Physics*, vol. 46, no. 5, pp. 1988–1995, 1992.

[31] M. S. M. Nour El-Din and M. E. Solite, "The mass-number dependence studies for the multiplicity of shower particles produced in interactions of different projectiles with emulsion nuclei at 3.7 GeV/n in the framework of the modified Glauber models I and II," *Canadian Journal of Physics*, vol. 87, no. 8, pp. 945–956, 2009.

[32] E. H. Esmael, M. S. M. Nour El -Din, and M. Y. M. Hassan, "Elastic scattering and breakup effect analysis of ^{11}Be + ^{12}C at 38.4 MeV/nucleon," in *Proceedings of the 4th Conference on Nuclear and Particle Physics*, October 2003.

[33] W. H. Barkas, *Nuclear Research Emulsion*, vol. 1, Academic Press, New York and London, 1973.

[34] P. L. Jain, M. M. Aggarwal, M. S. El-Nagdy, and A. Z. Ismail, "Fission of Uranium Nuclei in Flight at Relativistic Energies," *Physical Review Letters*, vol. 52, no. 20, pp. 1763–1766, 1984.

[35] B. Anderson, I. Otterlund, and E. Stenlund, "General properties of hadron-nucleus reaction multiplicities," *Physics Letters B*, vol. 84, no. 4, pp. 469–472, 1979.

[36] E. Firu, V. Bradnova, M. Haiduc et al., "Study of peripheral collisions of ^{56}Fe at 1 a GeV/c in nuclear emulsion," *Romanian Reports in Physics*, vol. 63, no. 2, pp. 425–436, 2011.

[37] M. A. Jilany, "Electromagnetic dissociation of 3.7AGeV ^{24}Mg and ^{28}Si projectiles in nuclear emulsion," *Nuclear Physics A*, vol. 705, p. 477, 2002.

[38] V. Singh, B. Bhattacharjee, S. Sengupta, and A. Mukhopadhyay, "Estimation of Impact Parameter on event-by-event basis in Nuclear Emulsion Detector," 2004, https://arxiv.org/abs/nucl-ex/0412051.